Mater. Res. Soc. Symp. Proc. Vol. 841 © 2005 Materials Research Society R10.9.1/T6.9.1

Micro-Raman Mapping and Analysis of Indentation-Induced Phase Transformations in Germanium

Jae-il Jang [1], M.J. Lance [2], Songqing Wen [1], J.J. Huening[3], R.J. Nemanich[3], and G.M. Pharr [1,2]
[1] The University of Tennessee, Dept. of Mater. Sci. & Eng., Knoxville, TN 37996-2200, USA.
[2] Oak Ridge National Laboratory, Metals and Ceramics Division, Oak Ridge, TN 37831, USA.
[3] North Carolina State University, Dept. of Physics, Raleigh, NC 27695, USA.

ABSTRACT

Although it has been confirmed by diamond anvil cell experiments that germanium transforms under hydrostatic pressure from the normal diamond cubic phase (Ge-I) to the metallic β-tin phase (Ge-II) and re-transforms to Ge-III (ST12 structure) or Ge-IV (BC8 structure) during release of the pressure, there are still controversies about whether the same transformations occur during nanoindentation. Here, we present new evidence of indentation-induced phase transformations in germanium. Nanoindentation experiments were performed on a (100) Ge single crystal using two triangular pyramidal indenters with different tip angles - the common Berkovich and the sharper cube-corner. Although the indentation load-displacement curves do not show any of the characteristics of phase transformation that are well-known for silicon, micro-Raman spectroscopy in conjunction with scanning electron microscopy reveals that phase transformations to amorphous and metastable crystalline phases do indeed occur. However, the transformations are observed reproducibly only for the cube-corner indenter.

INTRODUCTION

Together with silicon, germanium is one of the most important materials in the electronic industry, and thus its mechanical behavior is of a considerable interest from both scientific and engineering viewpoints. Following a number of theoretical studies and diamond anvil cell experiments (see review articles [1-2]), it is now well recognized that pristine Ge-I with its diamond cubic structure transforms to the metallic β-tin phase (Ge-II) at about 10 - 11 GPa, and, upon unloading, the Ge-II transforms to Ge-III (ST12, a simple tetragonal structure with 12 atoms in the unit cell) or Ge-IV (BC8, a body-centered cubic structure with 8 atoms in the unit cell), depending on the pressure release rate. Since these transformations are broadly analogous to those occurring in silicon, one might expect the well-known indentation-induced phase transformations for silicon to also occur in Ge. The structural similarities of these two materials also support this expectation. However, whether or not a phase transformation can actually occur during the nanoindentation of Ge is still controversial. While some experimental evidence for transformation has been reported for high load indentations performed mainly using a Vickers indenter [3-6], transformed phases have very rarely been observed reproducibly in Ge nanoindentations, as reviewed by Domnich and Gogotsi [1]. Moreover, using cross-sectional transmission electron microscopy, Bradby et al. [7] have found that severe twinning, rather than phase transformation, is the primary deformation mechanism in the spherical nanoindentation. As a result, they have suggested that, unlike Si, the hardness of Ge is not determined by the

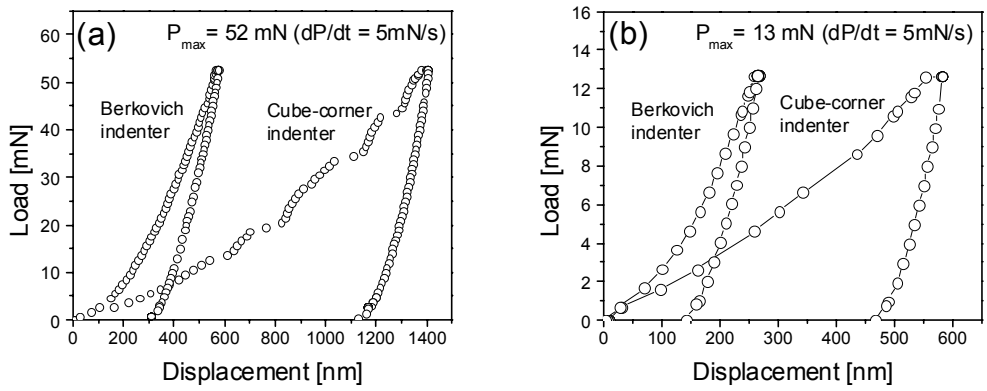

Figure 1. Nanoindentation load-displacement curves made in (100) Ge with cube-corner and Berkovich indenters at different peak loads; P_{max} = (a) 52 mN and (b) 13 mN.

phase transformation pressure. Very recently, Patriarche et al. [8] found the Ge-I and Ge-III (ST12) phases form in the residual indents of a-Ge thin films as observed in plan-view transmission electron microscopy. However, these phases result from what is probably an entirely different process involving the indentation-induced crystallization of an amorphous material. The current study was undertaken to explore other possible evidence for nanoindentation-induced phase transformation in Ge.

EXPERIMENTAL DETAILS

Nanoindentations were made on a standard (100) wafer Ge using a Nanoindenter-XP (MTS System Corp., Oak Ridge, TN). Based on the observation that a wide variety of transformation behaviors are observed in Si depending on indenter sharpness [9], two triangular pyramidal indenters were employed - the Berkovich and cube-corner indenters which have centerline-to-face angles of 65.3° and 35.3°, respectively. Indentation peak loads were varied in the range 10 to 100 mN at a fixed loading/unloading rate of 5 mN/sec. After nanoindentation testing, micro-Raman analyses were conducted within one hour using a Dilor XY800 Microprobe (JY Inc., Edison, NJ) and an Ar^+ laser operating at an excitation line of 5145 Å. To systematically characterize any new crystalline and amorphous phases that may have formed during indentation, Raman spectral maps of the indents were acquired using mapping software and a mesh size of 1 μm × 1 μm. The beam intensity was kept low to avoid possible artifacts induced by laser heating. All the hardness impressions were imaged using a Leo 1525 field-emission scanning electron microscope (SEM) (Carl Zeiss SMT Inc, Thornwood, NY) to identify important topographical features.

RESULTS AND DISCUSSION

Figure 1 shows examples of load-displacement (P-h) curves typically observed during nanoindentation with the cube-corner and Berkovich indenters. The sharper cube-corner

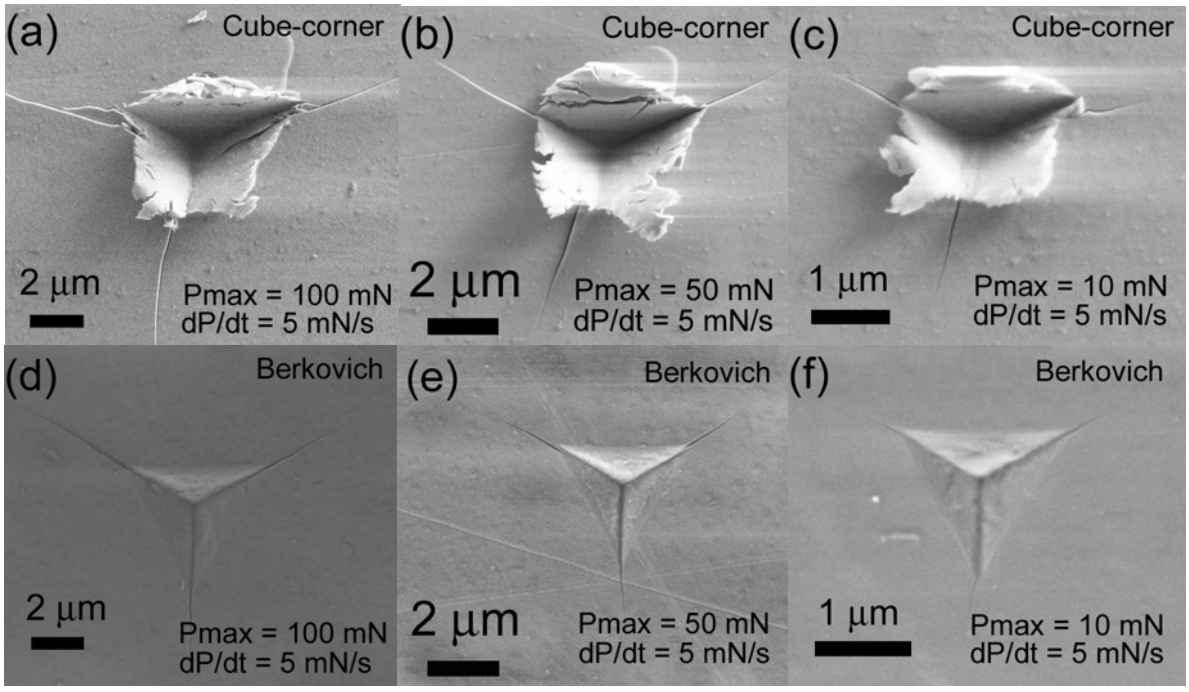

Figure 2. SEM micrographs of nanoindentation hardness impressions in (100) Ge, made at different indentation loads with (a)-(c) cube-corner indenter and (d)-(f) Berkovich indenter; Indentation peak load (Pmax): (a) and (d) 100 mN; (b) and (e) 50 mN; (c) and (f) 10 mN. Note that magnifications of the micrographs are not all the same.

indentations exhibit a higher displacement at peak load and a larger proportion of irreversible plastic deformation than the Berkovich indentations. When compared to similar curves for silicon, the most noteworthy feature is the lack of any unusual features in the unloading curve, particularly the "pop-out" and "elbow" behaviors. A number of pop-ins (discontinuities in loading sequence) are observed for the cube-corner indentations, especially at high loads. These most likely correspond to cracking and chipping rather than transformation since Ge has a very low fracture toughness, 0.6 $MPa(m)^{1/2}$, about half that of silicon. The P-h curves of indentations performed at loads lower than the first pop-in load (figure 1(b)) exhibited a large amount of plasticity, which would not be expected if the pop-ins corresponded to the initiation of phase-transformation-controlled indentation deformation.

The first solid evidence for phase transformation phenomena was found in SEM observations, as shown in figure 2. In the case of cube-corner indentations (figures 2(a) – 2(c)), thin, extruded material exhibiting metal-like plastic flow behavior is clearly seen at the contact periphery. Since such behavior is possible only when a thin layer of highly plastic material is sandwiched between the diamond indenter and the relatively hard surrounding Ge-I, the extrusions are direct evidence for the presence of a metallic-like phase such as Ge-II. Although this extrusion is well recognized in silicon since Pharr et al. first reported it in 1991 [10], it has not been observed in Ge. In contrast to cube-corner indentations, Berkovich indentations (figures 2(d) – 2(f)) showed no extruded material, although unusual deformed zones with a rough mottled appearance were observed within the hardness impressions. It has been suggested that these deformed zones represent the transformation from Ge-I to Ge-II [11], but it is difficult to state conclusively

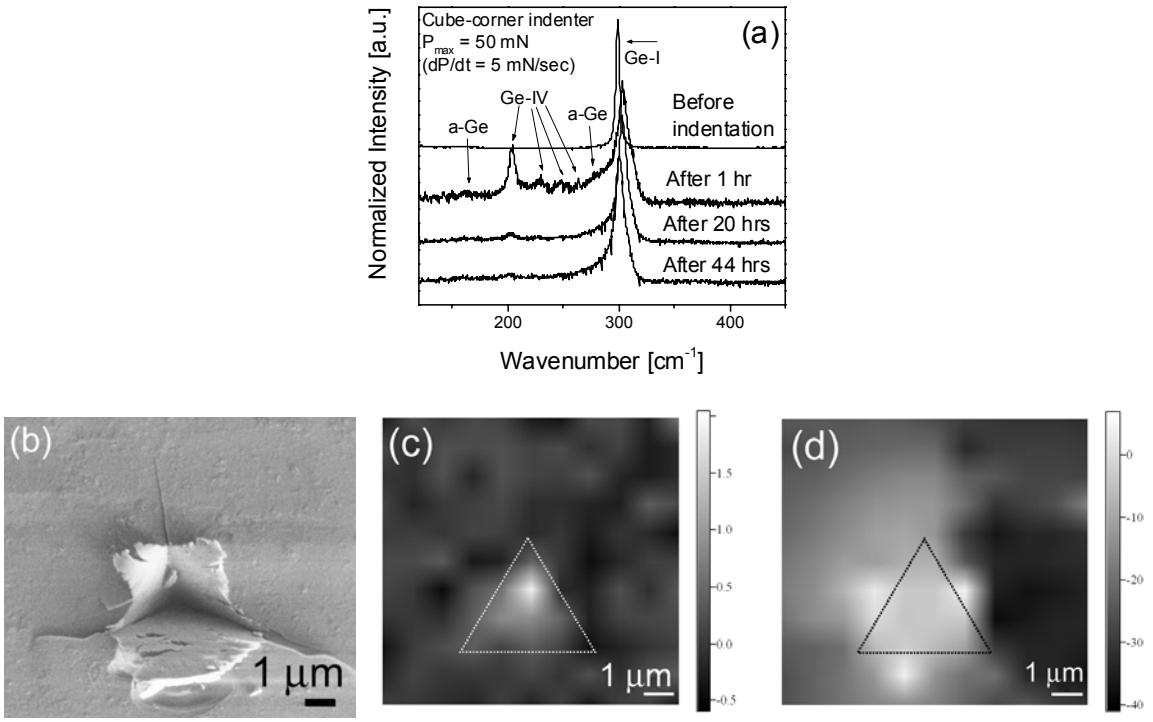

Figure 3. Results from cube-corner indentations made at P_{max} = 50 mN and dP/dt = 5 mN/sec: (a) typical Raman spectra; (b) SEM image; (c) micro-Raman map identifying the location of the transformed crystalline phase Ge-IV; (d) micro-Raman map identifying the location of the amorphous phase. In (c) and (d), the lighter regions correspond to the phase used to create the map. Creating these maps was started from 1 hour after the indentation test. Note that, in the Raman data, the Ge-IV phase was tentatively identified.

that the zones were formed by transformation rather than other deformation mechanisms such as twinning- or dislocation-mediated plasticity under highly constrained deformation conditions.

Additional strong evidence for the transformation was obtained through micro-Raman spectroscopy, as shown in figure 3(a). While pristine Ge-I exhibits only one sharp peak at 300 cm^{-1}, the micro-Raman spectra measured within one hour after cube-corner indentation show many narrow peaks at 205, 230, 250, and 264 cm^{-1} and broad bands around 150 and 270 cm^{-1}. The broad bands can be identified as amorphous Ge [6, 8], but the narrow peaks between 200 and 270 cm^{-1} represent a new crystalline phase. The peaks are very similar to ones observed during diamond anvil experiments by Hanfland and Syassen [12], who pointed out that they are strikingly similar to those for BC8-Si (Si-III). For this reason, we tentatively identify them as Ge-IV, for which the Raman spectrum is not currently known. Further examination of figure 3(a) shows that the peaks diminish substantially within 20 hours and are virtually absent after 44 hours. This is consistent with the observations of Nelmes et al. [13], who reported using synchrotron x-ray diffraction that the Ge-IV phase produced in diamond anvil cell experiments vanishes within 17 hours at room temperature and ambient pressure. By making micro-Raman maps with either the amorphous peak or the Ge-IV peak, the spatial locations of each of these phases are shown in figures 3(c) and 3(d). Comparing these maps with the SEM micrograph of

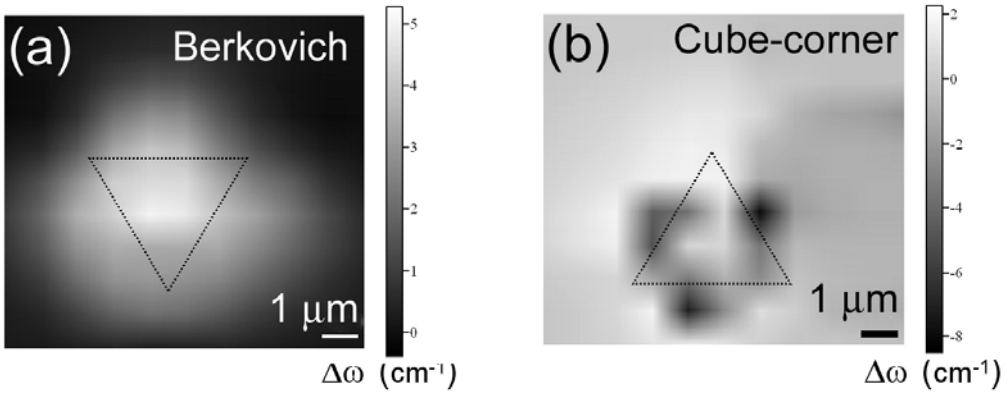

Figure 4. Micro-Raman maps showing the shift of the Ge-I peak: (a) Berkovich indentation and (b) cube-corner indentation. Both indentations were performed to a peak load of 50 mN at a loading/unloading rate of 5 mN/sec.

figure 3(b) shows that the extruded material is predominantly a-Ge, and the Ge-IV resides near the center of the hardness impression.

For Berkovich indentations made under similar loading conditions (not shown here), no crystalline peaks except for Ge-I were typically observed, although occasionally a peak corresponding to a-Ge or the Ge-IV phase was identified. These results are in agreement with those of Gogotsi et al. [14], who sometimes, but not reproducibly, could find crystalline Raman peaks for metastable phases in Berkovich indentations made at a high loading rate.

Another interesting observation is shown in the micro-Raman maps of Berkovich and cube-corner indentations in figure 4, which were constructed based on the frequency shift ($\Delta\omega$) of the primary Ge-I peak. This shift is directly related to the local residual stress; shifts to higher frequencies correspond to compressive stresses and lower frequencies to tensile stresses. The map for the Berkovich indentation in figure 4(a) reveals that the residual stresses within the indent are primarily compressive. Curiously, however, the image of the cube-corner indentation in figure 4(b) suggests that there are large tensile stresses near the contact periphery where the extrusions are observed. Since the extruded material is expected to be almost free of stress due to its thin geometry, the shift to lower frequencies is probably not an indication of tensile residual stress but rather that the extrusions are comprised of nanocrystalline Ge-I, which may crystallize from the amorphous phase, either on its own at room temperature or as activated by Raman laser heating [6]. By combining this result with the map shown in figure 3(d), it appears that the extruded material consists of a mixture of a-Ge and nanocrystalline Ge-I. Detailed studies of this and other related phenomena are currently underway.

CONCLUSIONS

Results presented here show that pressure-induced phase transformations do indeed occur during nanoindentation of Ge, but the transformations take place reproducibly only when sharper indenters like the cube-corner are used. This suggests that the larger volume displaced by the cube-corner indenter is important in the transformation process, either by increasing the extent and magnitude of the hydrostatic pressures, or by increasing the shear stresses in a manner that

aids the transformation. To better understand the deformation mechanisms, cross-sectional TEM and experiments that can characterize the transformation process in-situ are desirable.

ACKNOWLEDGEMENTS

This research was sponsored by the National Science Foundation under grant number DMR-0203552, and by the Division of Materials Sciences and Engineering (SHaRE User Center), U. S. Department of Energy, under contract DE-AC05-00OR22725 with UT-Battelle, LLC. The authors wish to thank Dr. V. Domnich for providing helpful documents.

REFERENCES

1. V. Domnich and Y. Gogotsi, in *Handbook of Surfaces and Interfaces of Materials Vol. 2*, edited by H. S. Halwa (Academic Press, New York, 2001), p. 355.
2. A. Mujica, A. Rubio, A. Munoz, and R.J. Needs, *Rev. Modern Phys*. **75**, 863 (2003).
3. I. V. Gridneva, Y. V. Milman, and V. I. Trefilov, *phys. Stat. sol*. (a) **14**, 177 (1972).
4. O. Shinomura, S. Minomura, N. Sakai, and K. Asaumi, *Phil. Mag*. **29**, 549 (1974).
5. D. R. Clarke, M. C. Kroll, P. D. Kirchner, and R. F. Cook, *Phys. Rev. Lett*. **60**, 2156 (1988).
6. A. Kailer, K.G. Nickel, and Y.G. Gogotsi, *J. Raman. Spcetrosc*. **30**, 939 (1999).
7. J.E. Bradby, J.S. Williams, J. Wong-Leung, M.V. Swain, and P. Munroe, *Appl. Phys. Lett*. **80**, 2651 (2002).
8. G. Patriarche, E. Le Bourhis, M.M.O. Khayyat, and M.M. Chaudhri, *J. Appl. Phys*. **96**, 1464 (2004).
9. J.-I. Jang, M.J. Lance, S. Wen, T.Y. Tsui, and G.M. Pharr, *Acta Mater*. (in press).
10. G.M. Pharr, W.C. Oliver, and D.S. Harding, *J. Mater. Res*. **6**, 1129 (1991).
11. S.V. Hainsworth, A.J. Whithead, and T.F. Page, in *Plastic Deformation of Ceramics*, edited by R. C. Bradt, C. A. Brookes, and J. L. Routbort (Plenum, New York, 1995), p. 173.
12. M. Hanfland and K. Syassen, *High Pressure Res*. **3**, 242 (1990).
13. R.J. Nelmes, M.I. McMahon, N.G. Wright, D.R. Allan, and J.S. Loveday, *Phys. Rev. B* **48**, 9883 (1993).
14. Y.G. Gogotsi, V. Domnich, S.N. Dub, A. Kailer, and K.G. Nickel, *J. Mater. Res*. **15**, 871 (2000).